Journal of Physics: Conference Series

PAPER • **OPEN ACCESS**

Optimal hybrid power plants for electric vehicle charging demand

To cite this article: Cameron Irmas *et al* 2024 *J. Phys.: Conf. Ser.* **2767** 082015

Optimal hybrid power plants for electric vehicle charging demand

Cameron Irmas, Kaitlin Brunik, Caitlyn E. Clark

National Renewable Energy Laboratory, Golden, Colorado, USA

E-mail: `cameron.irmas@nrel.gov`

Abstract. Transmission constraints, increasing motivations to decarbonize, and concerns over peak electric vehicle (EV) load impacts on local grids have driven electric customers to consider behind-the-meter, hybrid power plant generation and storage at the distributed-grid level for EV charging. In this study, we develop capabilities to optimize hybrid power plant component capacities for EV charging. We then demonstrate these capabilities in a case study for Boulder, Colorado, using public EV charging data as well as wind and solar resource data.

Our results show system designs that balance the cost of energy with load-meeting and peak shaving performance. Within the case study, systems designed for wind, solar photovoltaic (PV), and storage resulted in lower cost of energy than those optimized for PV and storage only. This indicates that in areas where wind resource exists, hybrid power plants that include wind, PV, and battery assets can better meet EV charging loads (including peak loads that are prone to overloading local grids) than PV and battery assets alone. Future work to address limitations in this paper include extending cost modeling to include performance losses (e.g., based on operations or weather) and charging station costs to estimate levelized cost of charging, and quantifying uncertainty and error in our aggregation methods for estimating EV charging loads at the hourly timescale.

1. Introduction

The transformation of the U.S. power sector is driven by increasing electrification, reliance on variable renewable energy generation, and integration of distributed energy resources. Distributed energy resources—including behind-the-meter (BTM) assets like distributed wind turbines, solar photovoltaic (PV) panels, batteries, and emerging loads like electric vehicles (EVs) and their supply equipment—are becoming integral components of modern grid systems. As variable renewable energy and distributed energy resources become more prevalent, pressure on grid resources increases, leading to bidirectional power flows and voltage fluctuations that impact grid design, control, and operation and that can stress local grids [1].

By 2030, it is expected that over half of all new cars sold in the United States will be EVs, and light-duty vehicles are projected to consume up to 3,360% more electricity by 2035 than they do today [2]. Meeting EV charging demands will require more high-voltage transmission lines to transport electricity from rural wind and solar power plants to demand centers; smaller distribution lines and transformers for last-mile electricity delivery; and hardware such as inverters that enables energy feedback to the grid [3].

However, the U.S. transmission system is constrained, resulting in delays for renewable energy developers seeking interconnections and grid updates. These limitations have spurred interest in distributed grid-level generation and storage. Commercial and industrial customers, who have the ability to generate BTM power on-site, as well as distributed grids and rural electric cooperatives at the edge of the grid who can co-locate self-generation with EV charging seek solutions to generate and use renewable energy locally, keep costs low, and increase their energy independence.

Hybrid energy systems (hybrids) at the distributed level are one solution to avoiding grid constraints and variable renewable energy concerns to more reliably and cost-effectively meet local EV charging demand. Hybrids combine generation like wind and PV assets with storage and end uses, and have the ability to provide energy and ancillary grid services more reliably than any of the single technologies can alone. Additionally, hybrids provide an opportunity to share building and infrastructure costs, capture otherwise clipped energy, and take advantage of federal incentive stacking.

Previous work has reviewed the state of the art in EV charging using distributed renewable energy assets, mostly focused on grid support functionality (e.g., vehicle-to-grid, charging aggregation, fast-charging capabilities) [4; 5; 6; 7; 8], advanced control and charge management [9; 10; 11], and optimal placement of EV charging stations [12]. When considering optimal hybrid power plant design for EV charging, Becker et al. optimized the capacity of stationary batteries for an electric school bus fleet [13]. Muratori et al. [14] co-simulated electricity rates and vehicle charging load scenarios at thousands of U.S. locations to assess opportunities to reduce fast-charging costs by deploying on-site collocated PV and batteries. However, optimizing wind, PV, and battery capacities for EV charging on-site has not been fully explored.

There is a need for a tool that simulates and optimizes fully coupled hybrid design and control for EV charging at the distributed, BTM level. This study begins to address that need by developing EV charging capabilities in the Hybrid Optimization and Performance Platform (HOPP) to enable capacity optimization of wind, PV, and stationary battery assets on-site for EV charging.

2. Research Objectives

The objective of this study is develop a configurable and extensible method of modeling hybrids designed to support EV charging. The subtasks are as follows:

- Investigate the balance between minimizing levelized cost of energy (LCOE) and ensuring that the system reliably mitigates peak charging loads.
- Develop a study showcasing an optimized hybrid system for mitigating EV charging loads using peak shaving.
- Understand benefits, trade-offs, and trends associated with different combinations of generation and storage.

3. Methodology

3.1. Modeling Tools

This study builds on HOPP, a Python-based, component-level, open-source tool for simulation, design, and optimization of hybrid plants [15], including generation and storage technologies. HOPP's primary dependency for generation and financial modeling is PySAM, a Python wrapper for the System Advisor Model (SAM) [16].

3.2. Optimization Tools

To streamline system optimization tooling for HOPP, we implement a flexible capacity optimization framework using Multi-Disciplinary Analysis and Optimization (MDAO) principles via the OpenMDAO Python package [17]. This approach—designed for scalable optimizations involving multiple connected systems with their own computations and derivatives—focuses primarily on gradient-based optimization, with multiple solvers supported. For this implementation, we use the Interior Point Optimizer (IPOPT), an open-source solver designed for complex nonlinear optimization problems [18]. Analytic gradients are not available for HOPP simulations, so we use a forward finite difference method to determine gradient information, provided by IPOPT.

3.3. Optimal Sizing Method

The optimal sizing method incorporates a discretized sweep of battery capacities, optimizing for LCOE by varying solar and wind capacity. It presents bounds on wind and solar, as well as a constraint ensuring that desired peak loads are met. These peak loads, in turn, represent demand that exceeds a configurable threshold power. These are further described in the following optimization formula.

Electric vehicle charging demand ($\mathbf{D}$) is represented as an hourly time series, in kilowatts:

$$\mathbf{D} = [d_1, d_2, ..., d_{8760}]$$

Battery capacity, $C_{b,i}$ (kWh), is calculated for a range of values of h, in hours:

$$\begin{aligned} C_{b,i} &= P_b * h_i \\ h_i &\in [h^-, h^+] \end{aligned}$$

where P_b is the battery power. We perform a sweep such that for each $C_{b,i}$ we optimize for wind and solar capacity. The system sizing optimization is represented as:

$$\begin{aligned} \text{minimize} \quad & LCOE \\ \text{by varying} \quad & P_w, P_s \\ \text{subject to} \quad & \bar{L}_{miss} - \bar{L}^+_{miss} \leq 0 \\ & P_w^- \leq P_w \leq P_w^+ \\ & P_s^- \leq P_s \leq P_s^+ \end{aligned}$$

where P_w is the wind capacity, P_s is the solar capacity, and $\bar{L}_{miss}$ is the average missed load. The peak load, $\mathbf{L}$, is the subset of the demand that exceeds the power threshold for peak shaving:

$$\begin{aligned} &\mathbf{L} = \{d_i \in \mathbf{D} \mid d_i > P_{th}\} \\ &\mathbf{L} \in \mathbb{R}^n \end{aligned}$$

The average missed peak load, $\bar{L}_{miss}$, measured in kilowatt-hours, is the average difference between the load demand (the difference between the peak load and the power threshold for peak shaving) and hybrid generation for that time step:

$$\bar{L}_{miss} = \frac{1}{n}\sum_{i=1}^{n}(\ell_i - P_{th} - P_i)t$$

where ℓ_i represents the peak load at that time step, $t = 1$ represents the hourly time step, and P_i is the total hybrid generation after curtailment, such that the missed load is zero if the combination of wind, solar, and battery dispatch meets the desired load. The strategy determining this generation is outlined in the following section.

Journal of Physics: Conference Series **2767** (2024) 082015 doi:10.1088/1742-6596/2767/8/082015

3.4. HOPP Model
To model wind and PV energy generation, we used HOPP [19], which leverages PySAM [16; 20] and FLORIS [21] to calculate wind and solar performance and costs. Default PySAM PV panel, wind turbine, and inverter models were used in this study, as described in [22].

To represent EV charging and battery dispatch, we developed a peak shaving dispatch. With this strategy, the battery is charged during times of low demand—in this case, during the day—and discharged during peak demand, which is based on a preconfigured threshold [23; 24]. There are two primary scenarios for the implemented control scheme: peak and non-peak. In a peak scenario, where demand is above threshold P_{th}, non-dispatched generation and battery are used to meet the difference between the peak load and the threshold. If the generation is greater than the desired amount, the excess will be used to charge the battery, and any generation beyond that is curtailed. If generation is less than needed, the battery is dispatched to help meet the load. In the case where the combination of generation and dispatch is insufficient to meet the peak load, the missed load is recorded. In the non-peak scenario, generation is primarily used to charge the battery, with excess used to meet non-peak demand. In all cases, the charging and discharging rate is determined based on the power fraction between the desired power based on the scenarios above, and the maximum power capability of the battery. The lower and upper state of charge (SOC) bounds for the battery are 10% and 90%, respectively.

LCOE is calculated using PySAM, via the `SingleOwner` financial model. It includes capital and operational costs for the hybrid system (wind, solar, and battery), extrapolating the year of generation data to calculate LCOE based on an expected plant lifetime of 25 years. Note that the dynamics and costs of charging infrastructure are not represented in this analysis but are further discussed in Section 6.

The dispatch modeling approach introduces assumptions. The model operates on a configurable time window, in this case 24 hours, based on a perfect forecast. Therefore, neither forecasting uncertainties nor strategies used to manage them are represented in this analysis. Additionally, the peak shaving heuristic currently does not support grid charging for the battery. It also does not involve more detailed battery simulation of voltage, current, thermal effects, and detailed degradation. However, these aspects are simulated *a posteriori* based on the dispatch profile and included in the finances. For this simulation we utilize the `BatteryStateful` model in PySAM, and maintain its default configuration.

4. Case Study
We apply this method in a case study for Boulder, Colorado, which serves as an effective baseline due to its combination of wind and solar resources, as well as its accessible EV load data. The EV demand profile is generated using the EVI-Pro (Lite) web tool to represent a fleet of 1000 vehicles that primarily charge at night [25]. A week of EV charging demand is depicted in Figure 1. This load profile represents the common multi-modal charging scenario in which peak charging times correspond with primarily evening charging behavior (most often associated with owners returning home at night and charging their EVs) and secondarily, morning charging behavior. For resource data, we use wind and solar time series data from the Wind Integration National Dataset (WIND) Toolkit and National Solar Radiation Database (NSRDB) [26; 27] for the year 2012 (Figure 2).

Table 1 describes the optimization parameters for the case study. These values are chosen to address the evening peak load demand seen in Figure 1, and these parameters are configurable by the user to meet intended use cases. A potential challenge exists in the battery power parameter, P_b, value selection. We choose P_b to be roughly the same as the largest desired peak shaving load, in this case 600 kW [23]. Non-peak loads are loads that do not exceed this 600 kW threshold.

We repeated the optimization sweep for a solar/storage-only scenario, with the same case study parameters (save the h bounds, which are wider for the PV-only scenario), for comparison.

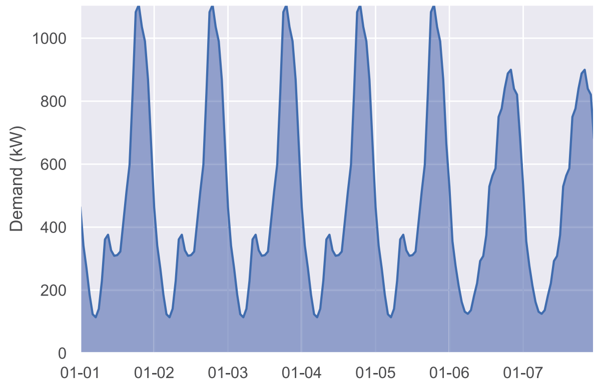

Figure 1: Hourly EV demand profile.

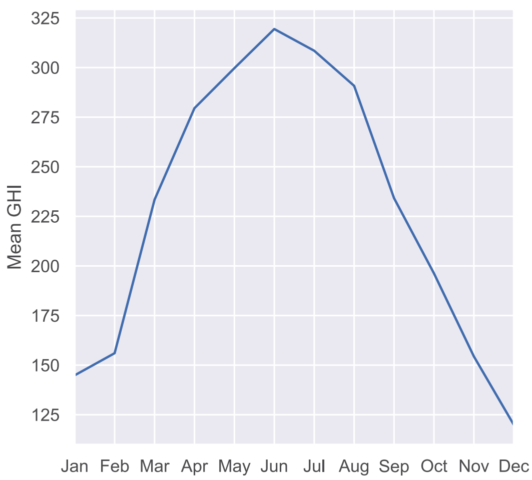

(a) Solar resource.

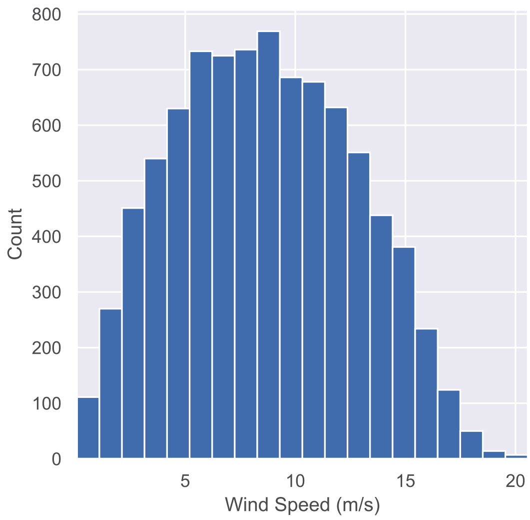

(b) Wind speed histogram.

Figure 2: Wind and solar resource.

Table 1: Parameters

Parameter	Description	Unit	Case Study Value/Range
P_b	Battery power	kW	600
h^-, h^+	Lower and upper bounds, battery duration	hours	[1,5]
P_{th}	Threshold power for peak shaving	kW	30
$\bar{L}^+_{\text{miss}}$	Upper bound on average missed load	kWh	500
P^-_w, P^+_w	Lower and upper bounds for wind capacity	kW	100, 1×10^6
P^-_s, P^+_s	Lower and upper bounds for solar capacity	kW	1×10^6

5. Results

5.1. Capacity Optimization Results

Sweep results are depicted in Figures 3 and 4. These show an optimal solution for minimizing the LCOE of a hybrid plant aimed at supporting EV charging loads. The plant's optimal capacities are a battery capacity of 1950.0 kWh, solar capacity of 446.16 kW, and wind capacity of 594.22 kW, resulting in an LCOE of $79.90/MWh. Wind and solar capacity both decrease with increased battery capacity, approaching 500 kW beyond the optimal point. LCOE initially decreases with increased battery capacity, but beyond the optimum, LCOE increases with battery capacity. For the plant without wind, the optimal capacities are a battery capacity of 3150.0 kWh and solar capacity of 1292.86 kW, resulting in an LCOE of $100.65/MWh.

The results from the sweep indicate stable convergence in hybrid system sizing. Increasing battery capacity leads to a decrease in wind and solar capacity, signaling efficient use of additional battery capacity and reduced reliance on non-dispatched generation. However, the extra battery capacity leads to higher system costs and overall LCOE, as the system relies more heavily on buffering and meeting the demand using battery power. This trade-off is further highlighted by the significantly higher LCOE for the system without wind. This system must rely on battery to manage peak loads, which occur at night: without support from wind generation, this increased battery size and utilization significantly increases costs.

Figure 5 demonstrates the behavior of the constraint on average missed load. For both system types, the constraint is active for battery capacities up to their respective optimal points, then $\bar{L}_{miss}$ decreases monotonically beyond the optimal points. Both systems exhibit similar behavior in that designs with battery capacities higher than optimal can more comfortably achieve missed load values within the constraint boundaries. In the optimal system, this missed load translates to roughly 88% of the desired peak shaving met across the time series.

While this case study holds the average missed load bound $\bar{L}^{+}_{miss}$ constant, the developed software can explore systems with varying resilience requirements. In some cases, including public transportation systems or micro-grid applications, higher resilience needs may necessitate more battery storage [28]; thus, this software maintains a balance between cost and performance via its objective, constraints, and configurable parameters.

5.2. Optimal System Results

Figure 6 highlights a one-week window depicting the original demand and the demand after peak shaving using optimal system capacities. The shaded area represents the total demand shaved, based on the difference between the peak demand and the hybrid system generation, including dispatch (and after curtailment of excess generation, if applicable). Figure 7 depicts non-dispatchable generation and curtailment over the time period, and Figure 8 shows battery operation, including power and SOC.

This time period highlights features of the system and its load management strategy. In the first two days of the week, consistent wind and variable solar provide enough generation to cover most peak shaving; however, wind drops on 1-17, and the battery dispatches at the beginning of the evening as solar generation drops. As the wind picks up later that night, it supports the peak shaving requirement while also charging the battery. Note that another low-wind period occurs toward the end of the week, from 1-20 to 1-21. In both low-wind cases, the battery supports a much larger share of the load. Figure 6 demonstrates that these periods result in the system missing a portion of the required load as the battery reaches its lower bound of SOC, or 10%, and can no longer dispatch.

Curtailment is calculated based on the desired loads for peak and non-peak times. For this system, curtailment is highest during daytime periods of high wind and solar. During these periods, EV charging demand is low, the battery charges quickly, the desired demand is easily met, and the rest of the generation is curtailed. At night, curtailment is low, as the system is

Journal of Physics: Conference Series **2767** (2024) 082015 doi:10.1088/1742-6596/2767/8/082015

designed to use the combination of wind and battery dispatch to meet these peaks.

The optimal system meets 86% of the total peak shaving and non-peak loads across the time series, and 88% of peak shaving loads alone. While the system was not explicitly designed to meet the non-peak loads, these results follow from the same behavior shown in curtailment. Low daytime EV charging demand is easily met by non-dispatchable generation, even after charging the battery. The missed peak loads are driven by the $\bar{L}^+_{miss}$ constraint: on average, the missed load is 30 kWh, so we expect values below and above 30 kW to be common. To meet other resilience needs, users may select other configurations with higher capacity, as demonstrated in Section 5.1, or rerun the optimization with a lower value of $\bar{L}^+_{miss}$.

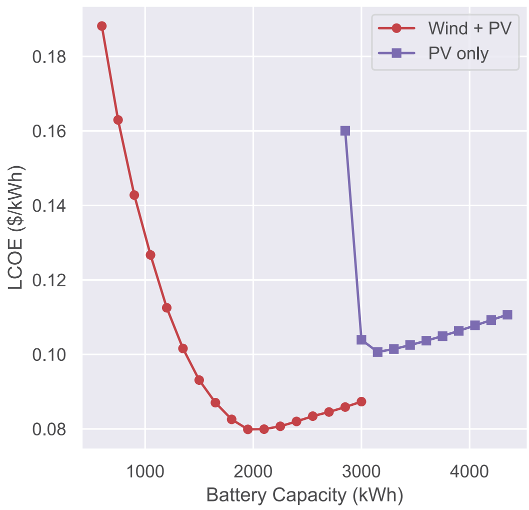

Figure 3: Sweep results: LCOE.

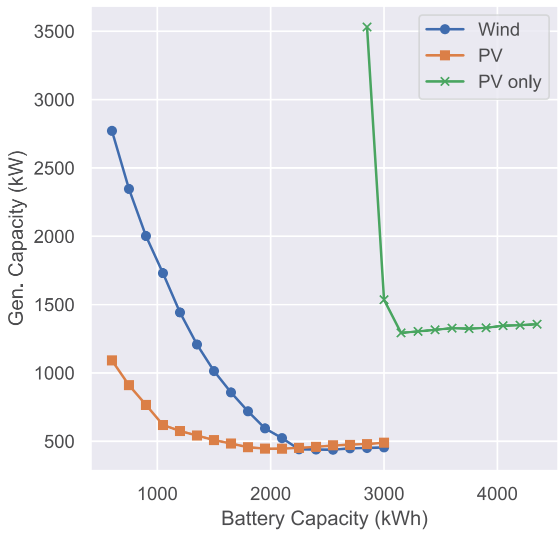

Figure 4: Sweep results: generation.

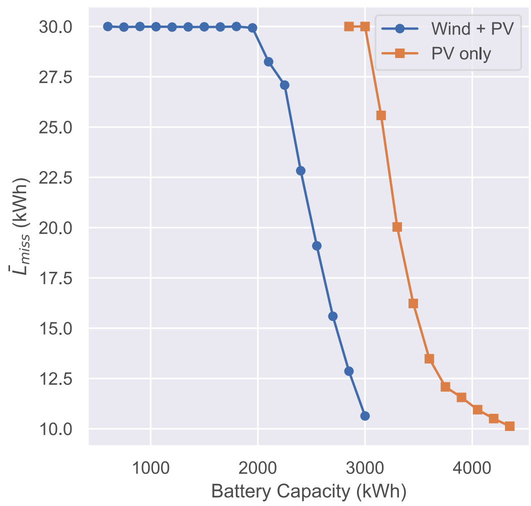

Figure 5: Average missed peak loads.

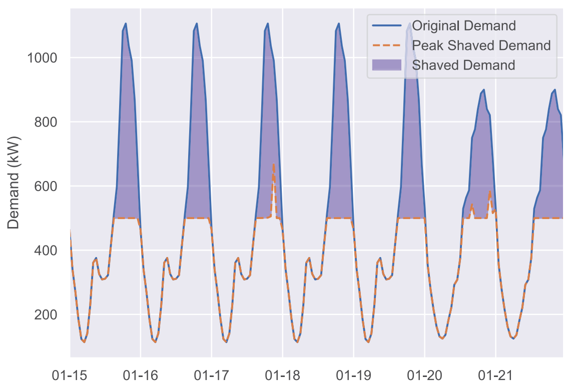

Figure 6: Peak shaving results.

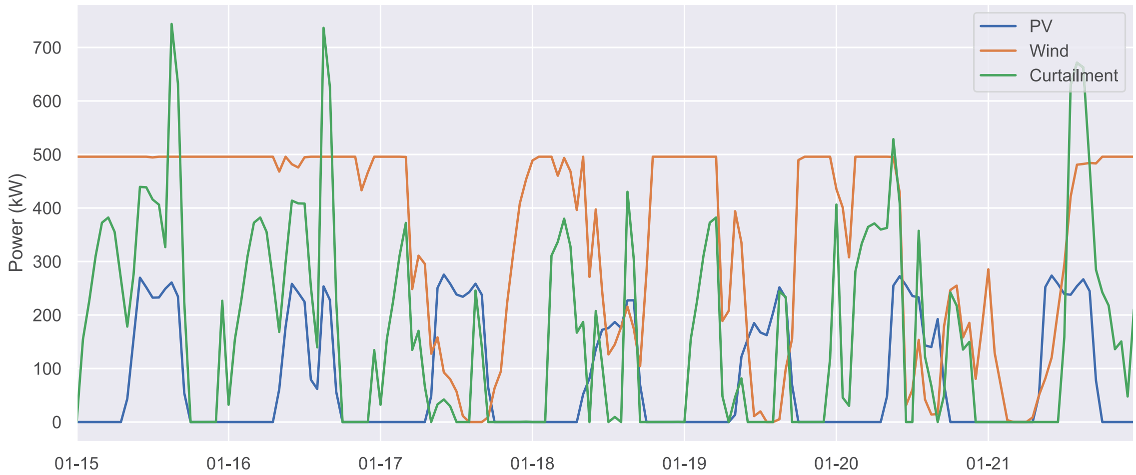

Figure 7: Generation and curtailment.

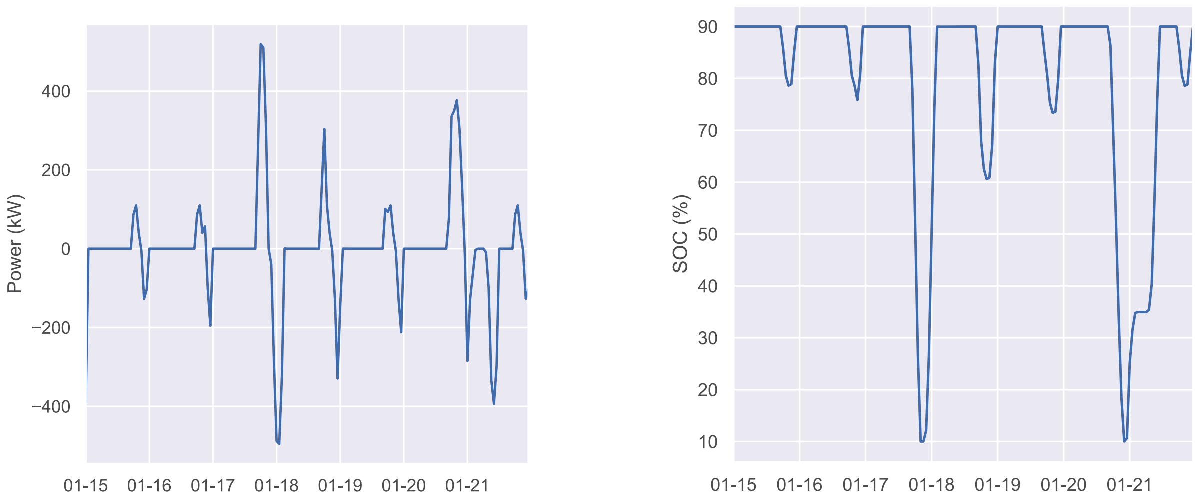

(a) Battery Power. (b) Battery SOC.

Figure 8: Battery operation.

6. Conclusions

EV adoption and the associated charging needs are set to add an increased strain on local distributed electric grids. Hybrid distributed BTM energy systems may alleviate that strain by collocating renewable energy generation and battery storage with EV charging demand, providing crucial power during peak loads, especially during times of low non-dispatchable generation.

To this end, we designed a configurable, foundational tool for sizing and simulating hybrid plants aimed at supporting EV charging. This includes a peak shaving battery dispatch strategy that prioritizes performance during peak loads—which typically occur at night when vehicles are charging—and prioritizes charging the battery outside of peak load times. It also implements a configurable optimization method that determines an optimal combination of wind, solar, and battery storage that minimizes LCOE while achieving desired peak shaving performance.

We further investigated the balance between LCOE and system performance, applying these new tools to a case study in Boulder, Colorado, using wind, solar, and EV load profile data. By comparing scenarios with and without wind, we identified that hybrid systems with wind power may allow for smaller systems that produce energy at lower cost while maintaining desired performance. Solar/storage-only systems must account for nighttime peaks by increasing the battery capacity and relying more heavily on battery utilization, driving up costs.

Future work will focus on a number of key areas. This study is limited in addressing the cost of energy, as it does not include the dynamics and costs of charging infrastructure, a significant cost [29]. By incorporating these elements, we may calculate levelized cost of charging (LCOC) and more thoroughly explore the financial feasibility of BTM systems for EV charging, potentially extending the optimization to use LCOC as an objective. Furthermore, including performance losses based on operations, weather, etc. will be important to sufficiently estimate LCOC. Alongside LCOC, other objectives, such as value of energy, which accounts for grid electricity price dynamics, could enable users to minimize cost to customers or developers. Additionally, optimal placement of a hybrid on the local grid is critical to minimizing grid impacts of EV charging. While HOPP is not a power flow analysis tool, it can be used alongside one to simulate a hybrid optimally placed and sized for meeting EV charging demands and reducing local grid impacts. Finally, this study aggregates EV charging demand data at a temporal resolution consistent with HOPP (hourly). However, EV charging loads are dynamic and often fluctuate significantly at the sub-hour timescale. Quantifying the impact of this aggregation for the results of a steady-state model like HOPP, and addressing any major disparities that arise, should be a topic of future work.

Acknowledgments

This work was authored by the National Renewable Energy Laboratory, operated by Alliance for Sustainable Energy, LLC, for the U.S. Department of Energy (DOE) under Contract No. DE-AC36-08GO28308. Funding provided by the U.S. Department of Energy Office of Energy Efficiency and Renewable Energy Wind Energy Technologies Office. The views expressed in the article do not necessarily represent the views of the DOE or the U.S. Government. The U.S. Government retains and the publisher, by accepting the article for publication, acknowledges that the U.S. Government retains a nonexclusive, paid-up, irrevocable, worldwide license to publish or reproduce the published form of this work, or allow others to do so, for U.S. Government purposes.

References

[1] Kroposki B, Bernstein A, King J, Vaidhynathan D, Zhou X, Chang C Y and Dall'Anese E 2020 *IEEE Power and Energy Magazine* **18** 37–46 ISSN 1540-7977 URL `https://ieeexplore.ieee.org/document/9229208/`

[2] McKerracher C, O'Donavan A, Soulopoulos N, Grant A, Lyu J, Mi S, Doherty D, Fisher R, Cantor C, Yang M, Ampofo K, Sekine Y, Leach A, Stoikou E, Shi J, Xu P, Yague L, Haring A, Geurts P, Adriaenssens C, Abraham A and Kareer K 2023 *BloombergNEF* 1–21 URL `https://about.bnef.com/electric-vehicle-outlook/`

[3] Plautz J 2023 *EE News by Poitico* 1–6 URL `https://www.eenews.net/articles/rural-utilities-turn-disruptive-as-they-embrace-renewables/`

[4] Ram S K, Devassy S, Verma B K, Mishra S and Akbar S A 2021 *2021 7th International Conference on Advanced Computing and Communication Systems, ICACCS 2021* 482–487

[5] Barman P, Dutta L, Bordoloi S, Kalita A, Buragohain P, Bharali S and Azzopardi B 2023 *Renewable*

and Sustainable Energy Reviews **183**(July) 113518 ISSN 18790690 URL https://doi.org/10.1016/j.rser.2023.113518

[6] Ntombela M, Musasa K and Moloi K 2023 *World Electric Vehicle Journal* **14**(7) ISSN 20326653

[7] Wu D, Aliprantis D C and Ying L 2012 *IEEE Transactions on Smart Grid* **3** 368–376 ISSN 1949-3061 conference Name: IEEE Transactions on Smart Grid URL https://ieeexplore.ieee.org/abstract/document/6009220

[8] Dallinger D and Wietschel M 2012 *Renewable and Sustainable Energy Reviews* **16** 3370–3382 ISSN 1364-0321 URL https://www.sciencedirect.com/science/article/pii/S136403211200113X

[9] Mohamed A A, Day D, Meintz A and Myungsoo J 2020 *Conference Proceedings - IEEE Applied Power Electronics Conference and Exposition - APEC* **2020-March** 873–878

[10] Mohamed A A, Jun M, Mahmud R, Mishra P, Patel S N, Tolbert I, Santhanagopalan S and Meintz A 2022 *IEEE Transactions on Transportation Electrification* **9**(4) 4951–4963 ISSN 23327782

[11] Mehrjerdi H 2021 *Journal of Energy Storage* **37** 102454 ISSN 2352-152X URL https://www.sciencedirect.com/science/article/pii/S2352152X2100205X

[12] Zhang M, Zhu X, Mather B, Kulkani P and Meintz A 2021 *2021 IEEE Power and Energy Society Innovative Smart Grid Technologies Conference, ISGT 2021*

[13] Becker W, Miller E, Mishra P P, Jain R, Olis D and Li X 2019 *51st North American Power Symposium, NAPS 2019* (March)

[14] Muratori M, Elgqvist E, Cutler D, Eichman J, Salisbury S, Fuller Z and Smart J 2019 *Applied Energy* **242**(March) 415–423 ISSN 03062619 URL https://doi.org/10.1016/j.apenergy.2019.03.061

[15] Tripp C, Guittet D, Barker A, King J and Hamilton B 2019 Hybrid optimization and performance platform (hopp)

[16] National Renewable Energy Laboratory PySAM URL https://sam.nrel.gov/software-development-kit-sdk/pysam.html

[17] Gray J S, Hwang J T, Martins J R R A, Moore K T and Naylor B A 2019 *Structural and Multidisciplinary Optimization* **59**(4) 1075–1104 URL http://www.umich.edu/~mdolaboratory/pdf/Gray2019a.pdf

[18] Wächter A and Biegler L T 2006 *Mathematical Programming* **106** 25–57 ISSN 0025-5610

[19] National Renewable Energy Laboratory 2023 Hybrid Optimization and Performance Platform (HOPP). Version 2.1.0 URL https://github.com/nrel/hopp

[20] Blair N, Diorio N, Freeman J, Gilman P, Janzou S, Neises T W and Wagner M J 2018 (NREL/TP-6A20-70414) URL https://www.nrel.gov/docs/fy18osti/70414.pdf

[21] National Renewable Energy Laboratory 2022 FLORIS. Version 3.1 - develop branch URL https://github.com/NREL/floris/tree/develop

[22] Clark C E, Barker A, King J and Reilly J 2022

[23] Oudalov A, Cherkaoui R and Beguin A 2007 Sizing and Optimal Operation of Battery Energy Storage System for Peak Shaving Application *2007 IEEE Lausanne Power Tech* pp 621–625 URL https://ieeexplore.ieee.org/abstract/document/4538388

[24] Lu C, Xu H, Pan X and Song J 2014 *Energies* **7** 8396–8410 ISSN 1996-1073 number: 12 Publisher: Multidisciplinary Digital Publishing Institute URL https://www.mdpi.com/1996-1073/7/12/8396

[25] Wood E URL https://www.osti.gov/biblio/1876634

[26] Draxl C, Clifton A, Hodge B M and McCaa J 2015 *Applied Energy* **151** 355–366 ISSN 03062619 URL http://dx.doi.org/10.1016/j.apenergy.2015.03.121

[27] Sengupta M, Xie Y, Lopez A, Habte A, Maclaurin G and Shelby J 2018 *Renewable and Sustainable Energy Reviews* **89** 51–60 ISSN 18790690 URL https://doi.org/10.1016/j.rser.2018.03.003

[28] Zhang M and Chen J 2014 *IEEE Transactions on Power Delivery* **29** 1427–1435 ISSN 1937-4208 conference Name: IEEE Transactions on Power Delivery URL https://ieeexplore.ieee.org/abstract/document/6814897

[29] Borlaug B, Salisbury S, Gerdes M and Muratori M 2020 *Joule* **4** 1470–1485 ISSN 2542-4351 URL https://www.sciencedirect.com/science/article/pii/S2542435120302312